Gamma decay studies of hypernuclei —Theoretical situation

D.J. Millener[a]

Brookhaven National Laboratory, Upton, NY 11973, USA

Abstract. Information on ${}^{7}_{\Lambda}$Li, ${}^{9}_{\Lambda}$Be, ${}^{10}_{\Lambda}$B, ${}^{11}_{\Lambda}$B, ${}^{12}_{\Lambda}$C, ${}^{15}_{\Lambda}$N, and ${}^{16}_{\Lambda}$O from the Ge detector array Hyperball is interpreted in terms of shell-model calculations that include both Λ and Σ configurations with p-shell cores. It is shown that the data puts strong constraints on the spin dependence of the ΛN effective interaction.

PACS. 21.80.+n Hypernuclei – 21.60.Cs Shell model

1 Introduction

The series of experiments using the Hyperball detector [1], which started in 1998 with KEK E419 [2,3] and BNL E930 [4], ended in 2005 with KEK E566 [5,6]. The last experiment, which used the upgraded Hyperball-2 detector, is still under analysis. This experiment on a ^{12}C target had as one objective the measurement of the ground-state doublet splitting in ${}^{12}_{\Lambda}$C by observing both γ rays from the excited 1^- level at ~ 2.6 MeV. At present, there is evidence for a 2667-keV γ ray associated with the $1^- \rightarrow 2^-$ transition. The second objective was to observe the ground-state doublet transition in ${}^{11}_{\Lambda}$B following proton emission from the region of the p_Λ peak near 11 MeV in ${}^{12}_{\Lambda}$C. In fact, two γ rays from ${}^{11}_{\Lambda}$B are seen at 264 keV and 1483 keV. The latter γ ray is known to be from the $1/2^+$ state built on the 718-keV 1^+ state of the ^{10}B core. This then means that the 264-keV γ-ray, seen also in KEK E518 [1,7,8], can be identified with the $7/2^+ \rightarrow 5/2^+$ ground-state doublet transition in ${}^{11}_{\Lambda}$B.

In the last experiment at BNL, E930($'$01), the ground-state doublet spacing in ${}^{16}_{\Lambda}$O was measured to be 26 keV [9]. From shell-model calculations, this small spacing results from a strong cancellation between the contributions from the spin-spin and tensor components of the ΛN effective interaction [9] and thus provides a sensitive measure of the strength of the tensor interaction once the strength of the spin-spin interaction is fixed by other data. In the same experiment, three γ rays from ${}^{15}_{\Lambda}$N are observed [1,10]. A 2268-keV γ ray has been interpreted as the transition from the $1/2^+;1$ level based on the 2313-keV $0^+;1$ level of ^{14}N to the $3/2^+$ member of the ground-state doublet [11,10]. The absence of the transition to the $1/2^+$ member of the ground-state doublet has been attributed to the weakness of the core M1 transition and further cancellations in the hypernuclear M1 matrix element [11,12]. The other two ${}^{15}_{\Lambda}$N γ rays, with energies of 1961 keV and 2442 keV, are interpreted as transions from the two members of the exited-state doublet based on the 3948-keV $1^+;0$ state on ^{14}N to the $1/2^+;1$ level [1,10], giving a separation of 481 keV for the doublet. Finally, there is evidence for a 6758-keV transition from the 2^- member of the upper doublet in ${}^{16}_{\Lambda}$O to the 1^- member of the ground-state doublet [10]. The spacing of the upper doublet is then 224 keV.

The ground-state doublet separation in ${}^{11}_{\Lambda}$B, the excited-state doublet separation in ${}^{15}_{\Lambda}$N, and the excited-state doublet separation in ${}^{16}_{\Lambda}$O all receive dominant contributions from the spin-spin component of the ΛN effective interaction (assisted by the effect of Λ–Σ coupling). These newly determined doublet spacings all indicate that the matrix element Δ of the spin-spin interaction should be smaller for hypernuclei in the latter half of the p shell than it is for ${}^{7}_{\Lambda}$Li.

In the following sections, the data on p-shell hypernuclei is interpreted in terms of shell-model calculations that include both $p^n s_\Lambda$ and $p^n s_\Sigma$ configurations in the basis [11,12]. As usual, the ΛN effective interaction is written [13–16]

$$\begin{aligned} V_{\Lambda N}(r) \;&=\; V_0(r) + V_\sigma(r)\; \boldsymbol{s}_N \cdot \boldsymbol{s}_\Lambda + V_\Lambda(r)\; \boldsymbol{l}_{N\Lambda} \cdot \boldsymbol{s}_\Lambda \\ &\quad + V_{\rm N}(r)\; \boldsymbol{l}_{N\Lambda} \cdot \boldsymbol{s}_N + V_{\rm T}(r)\; S_{12}\;, \end{aligned} \tag{1}$$

where $S_{12} = 3(\boldsymbol{\sigma}_N \cdot \hat{\boldsymbol{r}})(\boldsymbol{\sigma}_\Lambda \cdot \hat{\boldsymbol{r}}) - \boldsymbol{\sigma}_N \cdot \boldsymbol{\sigma}_\Lambda$. The five $p_N s_\Lambda$ two-body matrix elements depend on the radial integrals associated with each component in (1), conventionally denoted by the parameters $\overline{V}$, Δ, S_Λ, S_N and T [13]. The Λ–Σ coupling matrix elements between $p_N s_\Lambda$ and $p_N s_\Sigma$ states can be parametrized in the same way with the parameters denoted by a prime [11,12].

2 The ${}^{7}_{\Lambda}$Li hypernucleus

The first Hyperball experiment [2] established that ${}^{7}_{\Lambda}$Li should have five bound states below the ${}^{5}_{\Lambda}$He + d thresh-

[a] e-mail: millener@bnl.gov

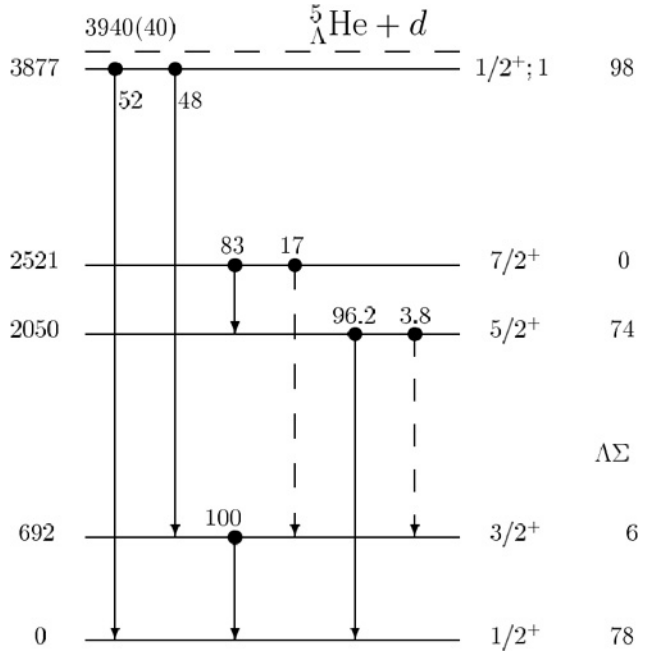

Fig. 1. The spectrum of $^7_\Lambda$Li determined from experiments KEK E419 and BNL E930 with the Hyperball detector. All energies are in keV. The energies of the excited $3^+;0$ and $0^+;1$ levels of the ^{6}Li core are 2186 and 3563 keV. The solid arrows denote observed γ-ray transitions. The γ-ray branching ratios are theoretical and the dashed arrows correspond to unobserved transitions. For each state of $^7_\Lambda$Li, the calculated energy shifts due to Λ–Σ coupling are given [18].

old at 5.94 MeV and observed four γ-ray transitions involving three excited states. The level scheme shown in Fig. 1 was completed when the $7/2^+ \rightarrow 5/2^+$ transition in the excited-state doublet was observed in coincidence with $5/2^+ \rightarrow gs$ transition following ^{3}He emission from $^{10}_\Lambda$B produced via the (K^-,π^-) reaction [17]. The energy spacings between levels of $^7_\Lambda$Li calculated with the parameter set (parameters in MeV)

$$\Delta = 0.430 \quad S_\Lambda = -0.015 \quad S_N = -0.390 \quad T = 0.030 \tag{2}$$

are given in Table 1. The two important central interaction parameters (in MeV) for the Λ–Σ coupling are [11,12]

$$\overline{V}' = 1.45 \quad \Delta' = 3.04\,. \tag{3}$$

The two doublet spacings are mainly due to the spin-spin interaction, augmented by the contribution from Λ–Σ coupling. These are the only contibutions to the ground-state doublet separation in the LS limit (the ^{6}Li ground-state wave function is mainly ^{3}S). The spacing of the excited-state doublet, based on the pure ^{3}D 3^+ state, is reduced by significant contributions from S_Λ and T. A substantial value for S_N is required to bring the $5/2^+$ and $1/2^+;1$ levels down to their observed energies. Note that the $3/2^+$ and $7/2^+$ levels are not strongly populated in the ^{7}Li(π^+,K^+) $^7_\Lambda$Li reaction [18] because they have predominantly intrinsic spin S = 3/2.

Table 1. Energy spacings in $^7_\Lambda$Li. The contributions from the 3^+ and $0^+;1$ core levels to the spacings are 2186 and 3563 keV. The first line in each case gives the coefficients of each of the ΛN effective interaction parameters as they enter into the spacing while the second line gives the actual energy contributions to the spacing in keV.

J^π_i/J^π_f	$\Lambda\Sigma$	Δ	S_Λ	S_N	T	ΔE
$\frac{3}{2}\,1^+/\frac{1}{2}\,1^+$		1.461	0.038	0.011	−0.285	
	72	628	−1	−4	−9	693
$\frac{5}{2}\,1^+/\frac{1}{2}\,1^+$		0.179	−1.140	0.738	1.097	
	4	77	17	−288	33	2047
$\frac{1}{2}\,2^+/\frac{1}{2}\,1^+$		0.972	−0.026	0.211	−0.085	
	−20	418	0	−82	−3	3886
$\frac{7}{2}\,1^+/\frac{5}{2}\,1^+$		1.294	2.166	0.020	−2.380	
	74	557	−32	−8	−71	494

3 The $^9_\Lambda$Be hypernucleus

The $3/2^+$ and $5/2^+$ members of the doublet based on the broad ($\Gamma \sim 1.5$ MeV) 3.03 MeV 2^+ state of ^{8}Be are expected to be roughly equally populated in (K^-,π^-) or (π^+,K^+) reactions. A reanalysis [8] of the original BNL E930 data [4] obtained γ-ray energies of 3024 and 3067 keV, leading to a separation energy of 43(5) keV. The breakdown of the doublet splitting for a calculation using the parameters of (2) and (3) is given in Table 2. In the LS limit for ^{8}Be, the 2^+ wave function has L = 2 and S = 0. Then, only the coefficient of S_Λ survives and takes the value −5/2. In the realistic case (< 5% admixture of configurations with S = 1), the contributions of S_Λ and T work against those from Δ and the Λ–Σ coupling (only 4, 2, and 10 keV for the $1/2^+$, $5/2^+$, and $3/2^+$ states because the Σ has to be coupled to T = 1 states of the core with a different symmetry from the T = 0 states). Looked at another way, one can see that the contributions brought in by the S = 1 admixtures tend to cancel and that the spacing is still a sensitive measure of S_Λ, which is constrained to be very small.

The parameter set chosen puts the $3/2^+$ state above the $5/2^+$ state but the order is not determined in the experiment. However, in the 2001 run of BNL E930 on a ^{10}B target, only the upper level is seen strongly following proton emission from $^{10}_\Lambda$B [8]. It can then be deduced that the $3/2^+$ state is the upper member of the doublet [11,12].

Table 2. Contributions from Λ–Σ coupling and the spin-dependent components of the effective ΛN interaction to the $3/2^+$, $5/2^+$ doublet spacing in $^9_\Lambda$Be. As in Table 1, the first line gives the coefficient of each parameter and the second line gives the actual energy contributions in keV.

$\Lambda\Sigma$	Δ	S_Λ	S_N	T	ΔE
	−0.033	−2.467	0.000	0.940	
−8	−14	37	0	28	44

4 The $^{16}_{\Lambda}$O hypernucleus

The proton threshold in $^{16}_{\Lambda}$O is at about 7.8 MeV. Thus, the members of the 1^-, 2^- doublet built on the 6176-keV $p_{3/2}$-hole state of ^{15}O are expected to be bound. The aim of BNL E930($'01$) was to observe γ-rays from the excited 1^- state to both members of the ground-state doublet and thus measure the doublet splitting. The population of the excited 1^- state is optimized by selecting pion angles near the maximum, at about 9°, of the $\Delta L = 1$ angular distribution in the (K^-, π^-) reaction [19]. The doublet splitting is of interest because it depends strongly on the tensor interaction. For a pure $p_{1/2}^{-1} s_\Lambda$ configuration, the combination of parameters governing the doublet splitting is [14]

$$E(1_1^-) - E(0^-) = -\frac{1}{3}\Delta + \frac{4}{3}S_\Lambda + 8T\ . \qquad (4)$$

The measured values of the γ-ray energies [9] are 6533.9 keV and 6560.3 keV (with errors of ~ 2 keV), giving 26.4 keV for the splitting of the ground-state doublet. Including recoil corrections of 1.4 keV to the γ-ray energies gives 6562 keV for the excitation energy of the 1^- state.

Since Ref. [9] was published, another peak, with a statistical significance of 3σ, has been found at 6758 keV [5, 10]. The most likely interpretation is that it corresponds to the $2^- \rightarrow 1_1^-$ transition (the 2^- level has to be excited by a weak spin-flip transition). This puts the 2^- state at 6786 keV and implies a splitting of 224 keV for the excited-state doublet. This is smaller than the 292 keV obtained using the $^{7}_{\Lambda}$Li parameters in (2). Reducing Δ from 0.43 MeV to 0.33 MeV reduces the doublet splitting to 238 keV. As noted in the introduction, more evidence for a smaller value of Δ in the latter half of the p shell comes from doublet splittings in $^{15}_{\Lambda}$N and $^{11}_{\Lambda}$B (see later).

The breakdown of the contributions to the energy spacing in $^{16}_{\Lambda}$O from the shell-model calculation is given in Table 3 for the parameter set (in MeV)

$$\Delta = 0.330 \quad S_\Lambda = -0.015 \quad S_N = -0.350 \quad T = 0.0239. \qquad (5)$$

Starting with $\Delta = 0.33$ MeV, T was chosen to fit the measured ground-state doublet spacing and S_N to fit the excitation energy of the excited 1^- level. The most important feature of the ground-state doublet splitting is the almost complete cancellation between substantial contributions from T and Δ (aided by Λ–Σ coupling). There is thus great sensitivity to the value of T if Δ is fixed from other doublet spacings.

Table 3. Energy spacings in $^{16}_{\Lambda}$O. The contribution of the core level spacing to the separation of the 1^- states is 6176 keV. The first line in each case gives the coefficients of each of the ΛN effective interaction parameters as they enter into the spacing while the second line gives the actual energy contributions to the spacing in keV.

J_i^π / J_f^π	$\Lambda\Sigma$	Δ	S_Λ	S_N	T	ΔE
$1^-/0^-$		−0.372	1.369	−0.003	7.883	
	−29	−123	−21	1	188	27
$1_2^-/1_1^-$		−0.256	−1.239	−1.494	−0.769	
	−32	−84	19	523	−18	6535
$2^-/1_2^-$		0.627	1.369	−0.003	−1.752	
	82	207	−21	1	−41	238

5 The $^{15}_{\Lambda}$N hypernucleus

At small angles in the ^{16}O$(K^-, \pi^-)^{16}_{\Lambda}$O reaction used for BNL E930, $p^{-1}p_\Lambda$ 0^+ states are strongly excited at about 10.6 and 17.0 MeV in excitation energy along with a broad distribution of $s^{-1}s_\Lambda$ strength centered near 25 MeV [20]. These levels can decay by proton emission (the threshold is at ~ 7.8 MeV) to $^{15}_{\Lambda}$N via $s^4p^{10}(sd)s_\Lambda$ components in their wave functions. The low-lying states of $^{15}_{\Lambda}$N can be populated by s-wave or d-wave proton emission and higher energy negative-parity states by p-wave emission.

Three γ-ray transitions, corresponding to the solid arrows in Fig. 2 have been observed [1,10]. The measured energies are 2268, 1961, and 2442 keV. The 2268-keV line is very sharp without Doppler correction, indicating a long lifetime compared to the stopping time in the target, and is identified with the transition from the $1/2^+;1$ level to the $3/2^+$ member of the ground-state doublet. The other two γ-ray lines are very Doppler broadened and therefore associated with states that have short lifetimes and it is natural to associate them with transitions from the upper

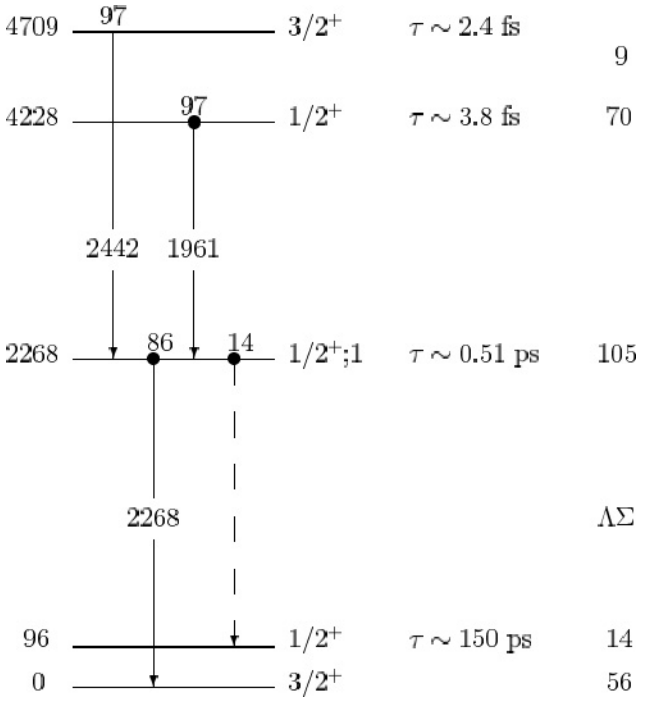

Fig. 2. The observed spectrum of $^{15}_{\Lambda}$N (except for the $1/2^+$ member of the ground-state doublet. All energies are in keV. The energies of the excited $0^+;1$ and $1^+;0$ levels of the ^{14}N core are 2313 and 3948 keV. The lifetimes and shifts due to Λ–Σ coupling, calculated using the parameters in (5), are shown on the right.

Table 4. Energy spacings in $^{15}_{\Lambda}$N. The core contributions to the energy spacings are derived from the excitation energies of the $0^+;1$ and $1^+;0$ states at 2313 and 3948 keV. The first line in each case gives the coefficients of each of the ΛN effective interaction parameters as they enter into the spacing while the second line gives the actual energy contributions to the spacing in keV. The first line of the table gives the coefficients for the ground-state doublet in the jj limit.

J_i^π/J_f^π	$\Lambda\Sigma$	Δ	S$_\Lambda$	S_N	T	ΔE
$p_{1/2}^{-2}$		0.5	−2.0	0	−12	
$\frac{1}{2}_1^+/\frac{3}{2}_1^+$		0.740	−2.237	0.024	−8.956	
	42	244	33	−8	−214	96
$\frac{1}{2}_2^+/\frac{3}{2}_1^+$		0.262	−0.752	0.016	−2.966	
	−50	86	11	−5	−71	2282
$\frac{1}{2}_3^+/\frac{3}{2}_2^+$		1.367	0.130	0.034	−0.424	
	61	451	−2	−12	−10	502
$\frac{3}{2}_2^+/\frac{1}{2}_2^+$		0.474	0.025	−1.335	−0.271	
	96	156	0	467	−6	2342

doublet in Fig. 2 because the $1^+;0 \rightarrow 0^+;1$ core transition is a fast M1. In fact, the 2442-keV transition is observed in coincidence with the 2268-keV γ ray [10].

The contributions to the energy spacings from a shell-model calculation using the parameters of (5) are given in Table 4. The tensor interaction in the p-shell Hamiltonian was kept fixed during a p-shell fit and was chosen to ensure cancellation in the Gamow-Teller matrix element for ^{14}C(β^-) decay, which is proportional to $\sqrt{3}a(^1S)\,a(^3S) + a(^1P)\,a(^3P)$ in (6). The relevant core wave functions are

$$\begin{aligned} |^{14}\mathrm{N}(0^+;1)\rangle &= \ \ 0.7729\ ^1S + 0.6346\ ^3P \\ |^{14}\mathrm{N}(1_1^+;0)\rangle &= -0.1139\ ^3S + 0.2405\ ^1P - 0.9639\ ^3D \\ |^{14}\mathrm{N}(1_2^+;0)\rangle &= \ \ 0.9545\ ^3S + 0.2958\ ^1P - 0.0390\ ^3D\ . \end{aligned} \quad (6)$$

The lowest 0^+ and 1^+ states are 93% and 85% $p_{1/2}^{-2}$, respectively. The entries for the ground-state doublet of $^{15}_{\Lambda}$N in Table 4 show a significant shift away from the jj-coupling limit (the coefficients are $-3/2$ times those in (4)) with the result that the higher-spin member of the doublet is predicted to be the ground state in contrast to the usual ordering for p-shell hypernuclei, including $^{16}_{\Lambda}$O.

In the weak-coupling limit, the branching ratio for γ-rays from the $1/2^+;1$ state is 2:1 in favor of the transition to the $3/2^+$ final state (the statistical factor from the sum over final states). However, the transition to the $1/2^+$ state is not observed despite the fact that the transition to the $3/2^+$ state is very clearly observed with over 700 counts [10]. In addition, a lifetime estimate for the $1/2^+;1$ level is 1.4 ps [10], which is very much longer than the 0.1 ps lifetime of $0^+;1$ level in ^{14}N. The essential reason, pointed out in Ref. [11] and in more detail in Ref. [12], is that small $1_2^+ \times s_\Lambda$ admixtures in the wave functions for the ground-state doublet members bring in a very strong M1 matrix element that cancels against the predominantly orbital M1 matrix element of the core transition. Even the small Σ admixtures contribute to the cancellation. The cancellation is stronger for the transition to the $1/2^+$ member of the ground-state doublet. The reason for this can be seen from Table 5. Namely, the largest contributions to the off-diagonal matrix elements come from S_N and T and add for the $1/2^+$ state and cancel for the $3/2^+$ state. The net effect is to increase the lifetime of the $1/2^+;1$ level in $^{15}_{\Lambda}$N by a factor of five over that of the $0^+;1$ core state. The data suggests that an even stronger cancellation takes place and this would further reduce the branching ratio for the $1/2^+;1 \rightarrow 1/2^+;0$ transition.

Table 5. Coefficients of the ΛN interaction parameters in the off-diagonal matrix elements between the $1_1^+;0\times s_\Lambda$ and $1_2^+;0\times s_\Lambda$ basis states in $^{15}_{\Lambda}$N and the 1^- states in $^{16}_{\Lambda}$O. The second line gives the energy contributions in MeV.

J^π	Δ	S_Λ	S$_N$	T	ME
$1/2^+$	0.1275	−0.1275	0.4581	−4.0664	
	0.0421	0.0019	−0.1603	−0.0972	−0.214
$3/2^+$	−0.0637	0.0637	0.4581	2.0332	
	−0.0210	−0.0010	−0.1603	0.0486	−0.134
1^-	0.4714	-0.4714	0.	1.4142	
	0.1556	0.0071	0.	0.0338	0.196

It should be mentioned that there is a puzzle concerning the γ-ray assignments in $^{15}_{\Lambda}$N. The yield of 2268-keV γ rays rises sharply with decreasing pion angle, as expected for s-wave proton emission from a 0^+ initial state to a $1/2^+$ final state [10]. The same behavior is observed for the 2442-keV γ ray but a $3/2^+$ assignment for the final state requires d-wave emission from an initial 0^+ state. This is expexted to be structurally hindered for a transition from an initial state with a mixture of $L = S = 0$ and $L = S = 1$ to a final state with a dominant $L = 0$, $S = 3/2$ component. Conversely, the yield of the 1961-keV γ ray does not rise at forward pion angles. The proton spectroscopic factors arise from the small $p^{10}(sd)s_\Lambda$ components in the $^{16}_{\Lambda}$O wave functions, which must be present from normal configuration mixing and to eliminate spurious center-of-mass components, and it remains to be seen whether large-basis shell-model calulations can explain the observed behavior.

6 The $^{11}_{\Lambda}$B hypernucleus

The lowest particle threshold (proton) in $^{11}_{\Lambda}$B is at 7.72 MeV and the ^{10}B core has many low-lying p-shell levels. This leads to the expectation that a considerable number of γ-ray transitions in $^{11}_{\Lambda}$B could be observed and thus provide tests of the parametrization of the ΛN effective interaction.

A shell-model calculation for $^{11}_{\Lambda}$B was made using the p-shell interaction of Barker [21], who made changes to the (6-16)2BME interaction of Cohen and Kurath [22] to improve the description of electromagnetic transitions in ^{10}B [23,24]. The strengths for formation via non-spin-flip transitions (on the left side of Fig. 3) and the electromagnetic matrix elements for decay were calculated for all the

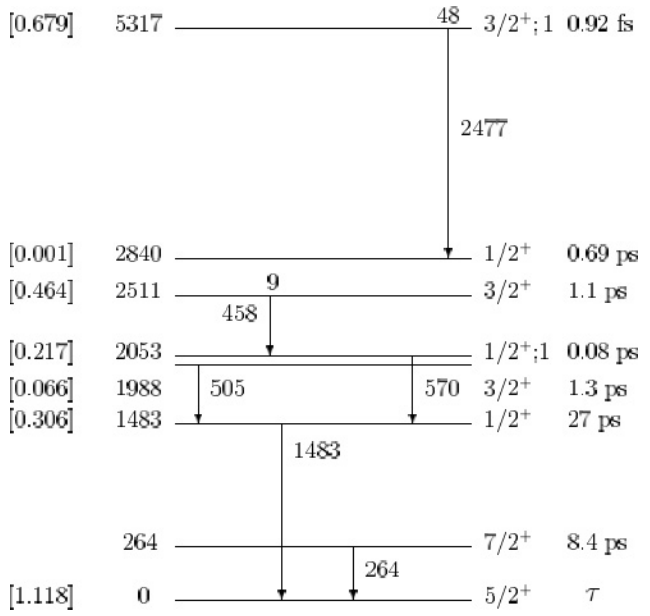

Fig. 3. The spectrum of $^{11}_{\Lambda}$B based on the six observed γ-ray transitions. All energies are in keV. The energies of the excited $1^+_1;0$, $0^+;1$, $1^+_2;0$, and $2^+;1$ levels of the ^{10}B core are 718, 1740, 2154, and 5164 keV. The placements of the 264-keV, 1482-keV, and 2477-keV transitions are well founded (see text). The placement of the other three γ-rays is more speculative. The formation factors for the (π^+, K^+) reaction on the left and the lifetimes on the right are from the shell-model calculation.

Table 6. Contributions of the spin-dependent ΛN terms to the binding energies of the eight levels of $^{11}_{\Lambda}$B shown in Fig. 3 given as the coefficients of each of the ΛN effective interaction parameters. The theoretical excitation energies and the gains in binding energy due to Λ–Σ coupling are given in keV.

$J^\pi;T$	E_x	$\Lambda\Sigma$	Δ	S_Δ	S_N	T
$5/2^+;0$	0	66	−0.616	−1.377	1.863	1.847
$7/2^+;0$	266	11	0.409	1.090	1.890	−1.512
$1/2^+;0$	968	71	−0.883	−0.116	0.746	0.243
$3/2^+;0$	1442	12	0.403	0.094	0.872	−0.194
$1/2^+;1$	1970	93	−0.007	0.008	1.543	−0.013
$3/2^+;0$	2241	46	−0.266	0.754	1.536	−1.264
$1/2^+;0$	2554	35	0.333	−1.333	1.674	2.639
$3/2^+;1$	5366	103	−0.203	−1.293	1.519	0.598

bound p-shell hypernuclear states of $^{11}_{\Lambda}$B (i.e, up to the states based on the 5.92-MeV $2^+;0$ level of ^{10}B). The γ-ray cascade was followed from the highest levels, summing the direct formation strength and the feeding by γ rays from above. The lowest $1/2^+;0$ level, originally predicted at 1.02 MeV, acts as a collection point for the γ-ray cascade. The conclusion was that perhaps as many as eight transitions would have enough intensity to be seen in an experiment with the Hyperball.

Table 6 gives the predicted excitation energies and a breakdown of the contributions for the parameter set (5). The p-shell core states all have dominant [42] spatial symmetry. The 1.74-MeV $0^+;1$ and 0.72-MeV $1^+;0$ states are mainly L = 0 while the 2.15-MeV $1^+;0$, 3.59-MeV $2^+;0$, and 4.77-MeV $3^+;0$ states form a L=2, S=1 triplet with $K_L = 0$. The $3^+;0$ gs, the 5.92-MeV $2^+;0$ state, and the 6.03-MeV $4^+;0$ state are mainly $K_L = 2$ with the lowest L value dominant and an ~ -0.35 admixture of the next L value. This corresponds to $K_J = 3$ for the 3^+ and 4^+ states, which are connected by a very strong E2 transition [25]. Selection rules involving the dominant L and K_L assignments put strong constraints on the M1 and E2 matrix elements involved in the γ-ray cascade.

The six transitions actually observed in KEK E518 [7] are tentatively placed in a decay scheme in Fig. 3 and their relative intensities and lifetime information are compared with the shell-model results in Table 7. The strongest γ ray in the spectrum was found at 1483 keV and it is very sharp implying a long lifetime. Despite the unexpectedly high energy compared with the prediction in Table 6, it is natural to associate this γ ray with the E2 de-excitation of the lowest $1/2^+;0$ level. The formation strengths on the left side of Fig. 3 show that the most strongly formed excited state is expected to be the $3/2^+;1$ level based on the 5.16-MeV $2^+;1$ state of ^{10}B. The 2477-keV γ ray that shows up after the Doppler-shift correction has a natural assignment as a strong (1.1 W.u.) isovector M1 transition between states with L=2 and K_L=0; the other major γ-ray branch (41%) feeds the 1483-keV level. The 264-keV line is now known [5,6] to be associated with the ground-state doublet transition (0.2 W.u.). The placement of the other three γ-ray transitions in Fig. 3 is speculative. The $1/2^+;1 \rightarrow 1/2^+;0$ transition is a 2.0 W.u. M1 transition between states with L = 0 giving a short lifetime for the initial level. The line is predicted to be the most intense one after the 1483-keV transition and is associated with the 570-keV γ ray rather than the 505-keV γ ray based on the lifetime information in Table 7. The assignments of the 458-keV and 505-keV γ rays are the least certain and could possibly be interchanged. This is because the $2154 \rightarrow 1740$ transition in ^{10}B is a relatively weak M1 transition [25] (L mismatch) and the mixing of the hypernuclear states based on the two $1^+;0$ core states brings in the strong $1740 \rightarrow 718$ M1 matrix element and destructive interference (cf. the situation for $^{15}_{\Lambda}$N).

Table 7. Comparison of measured relative intensities and lifetime information [7] with shell-model results for the six γ-ray transitions in $^{11}_{\Lambda}$B. The fourth column gives lifetimes including only statistical errors. The fifth column gives looser limits resulting from the inclusion of systematic errors and γ-ray cascade feeding.

E_γ (keV)	Relative Intensity		Lifetime (ps)		
	Exp.	Th.	Exp.	Exp.	Th.
264	0.14(3)	0.21	> 3.5	> 1.0	8.4
458	0.12(3)	0.05	$0.6^{+0.7}_{-0.3}$	< 1.6	1.1
505	0.28(5)	0.17	2.8(20)	> 0.9	1.3
570	0.23(5)	0.28	$0.5^{+1.0}_{-0.2}$	< 1.9	0.08
1483	1.00	1.00	> 15	> 6.0	27.0
2477	0.16(4)	0.25	< 0.2	< 0.5	0.0009

The most glaring discrepancy is that the shell-model calculation greatly underestimates the excitation energies of the two doublets based on the $1^+;0$ levels of ^{10}B. From Table 6, it can be seen that S_N does raise the energies of these doublets with respect to the ground-state doublet but not nearly enough. The shell-model calculation is in fact quite volatile with respect to the p-shell wave functions for the $1^+;0$ core levels (exacerbated by the fact that the isoscalar M1 transitions are weak). There is also mixing of the members of these two doublets and this is evident from the difference between the coefficients of S_N for the doublet members (they have to be the same in the weak-coupling limit).

The value for Δ of 0.33 MeV from (5) gives spacings of 474 keV and 313 keV for the doublets based on the 1^+ states (see Table 6). This puts the shell-model spacing for the first-excited doublet $(1/2^+_1;0,\ 3/2^+_1;0)$ in the range of the most likely assignments of 505 and 458 keV, unlike the original prediction of 653 keV (with $\Delta = 0.488$ MeV), and the smaller spacing for the second-excited doublet $(3/2^+_2;0,\ 1/2^+_2;0)$ limits the decay branch for the inter-doublet transition, tending to remove this transition as a candidate for the observed γ rays.

The effect of Barker's modifications [21] to the Cohen and Kurath interaction is to severely limit the L = 0/L = 2 mixing (to $\sim$ 2.2%) in the two lowest 1^+ states [24]. P-shell interactions with the tensor interaction constrained to fit ^{14}C β decay also restrict the L mixing and give similar results for $^{11}_{\Lambda}$B but many p-shell interactions produce considerable L mixing ($10-20\%$ is common). This reduces doublet spacings for both excited doublets, as can be deduced from Table 6 (the coefficients of Δ for the $3/2^+$–$1/2^+$ spacing are 3/2 and $-3/4$ for pure L = 0 and L = 2, respectively).

7 The $^{10}_{\Lambda}$B and $^{12}_{\Lambda}$C hypernuclei

The ^{9}B and ^{11}C core nuclei have a simlar structure with $3/2^-$ ground-states resulting from one particle or one hole in the K = 3/2 p-shell Nilsson orbit. Table 8 shows the similarity of the contributions from the ΛN interaction to the $2^-/1^-$ ground-state doublet separation for the parameter set (5). The most notable feature of Table 8 is that the Λ–Σ coupling increases the doublet spacing in $^{12}_{\Lambda}$C and reduces it in $^{10}_{\Lambda}$B. The reason for this is that spin-spin matrix element for the ΛN interaction depends on an isoscalar one-body density-matrix element of the nuclear spin operator for the core while the corresponding matrix element for Λ–Σ coupling depends on an isovector one-body density-matrix element of the nuclear spin operator for the core. The isoscalar and isovector matrix elements are both large but they have opposite relative sign for the two hypernuclei. The coupling matrix elements are broken down in Table 9. The "diagonal" matrix elements involving the $3/2^-$ core states contain a contribution of 1.45 MeV from $\overline{\mathrm{V}}'$ (3) and the contribution from Δ' produces the shifts from this value. If it were not for the contribution to the energy shifts from the $1/2^- \times \Sigma$ configuration (the $1/2^-$ and $3/2^-$ core states both have L = 1), there would be a much larger effect on the relative ground-state doublet spacings in $^{10}_{\Lambda}$B and $^{12}_{\Lambda}$C.

Table 8. Coefficients of the ΛN interaction parameters for the $2^-/1^-$ ground-state doublet separations of $^{10}_{\Lambda}$B and $^{12}_{\Lambda}$C. The energy contributions from Λ–Σ coupling and the doublet splitting ΔE are in keV.

	$\Lambda\Sigma$	Δ	S_Λ	S_N	T	ΔE
$^{12}_{\Lambda}$C	57	0.531	1.45	0.038	−1.77	150
$^{10}_{\Lambda}$B	−14	0.570	1.43	0.008	−1.10	121

Table 9. Matrix elements (in MeV) coupling Σ configurations with the members of the $3/2^- \times \Lambda$ ground-state doublets in $^{10}_{\Lambda}$B and $^{12}_{\Lambda}$C. The energy shifts caused by these couplings are given in keV.

	J^π	$3/2^- \times \Sigma$	$1/2^- \times \Sigma$	$\Lambda\Sigma$ shift
$^{10}_{\Lambda}$B	1^-	0.55	1.47	34
	2^-	1.95		49
$^{12}_{\Lambda}$C	1^-	1.92	−1.35	98
	2^-	1.13		40

The 2^- state of $^{10}_{\Lambda}$B is populated by non-spin-flip transitions from the 3^+ ground state of ^{10}B. The resulting γ-ray transition was first searched for in [26] without success, an upper limit of 100 keV being put on the doublet spacing (in BNL E930, the transition was also looked for and not found at roughly the same limit [1]). In $^{12}_{\Lambda}$C, it is the 1^- ground state that is populated by non-spin-flip transitions from a ^{12}C target and the doublet spacing is best investigated by looking for transitions from higher bound states of $^{12}_{\Lambda}$C. This approach was tried in KEK E566 and the data is still under analysis. The dominant contribution to the spacings arises from the spin-spin interaction and the coefficient of Δ is sensitive to the p-shell interaction through L mixing in the core ground state via the spin-orbit interaction. For L = 1, the coefficient of Δ is 2/3 whereas for L = 2 it is $-2/5$. For pure K = 3/2, the amplitudes for L = 1 and L = 2 are $\sqrt{21/26}$ and $-\sqrt{5/26}$ leading to a coefficient of Δ equal to $6/23 \sim 0.46$. As an example, the (8-16)2BME interaction of Ref. [22] gives a coefficient close to this value for $^{12}_{\Lambda}$C.

8 Summary and outlook

The era of Hyperball experiments at KEK and BNL between 1998 and 2005 has provided accurate energies for about 20 γ-ray transitions in p-shell hypernuclei, including 7 doublet spacings. With the exception of transitions in $^{11}_{\Lambda}$B that most likely involve levels based on the two lowest 1^+ states of ^{10}B, the γ-ray data can be accounted for by shell-model calculations that include both Λ and Σ configurations with p-shell cores. The spin-dependence of the effective ΛN interaction appears to be well determined with some dependence on nuclear size (or binding energy) that is reflected in the difference between the parameters in (2) for $^{7}_{\Lambda}$Li and in (5) for the heavier p-shell hypernuclei.

The singlet central interaction is more attractive than the triplet, as evidenced by the value $\Delta = 0.43$ MeV needed to fit the 692-keV ground-state doublet separation in ${}^{7}_{\Lambda}$Li (and the 471-keV excited-state doublet spacing). In ${}^{7}_{\Lambda}$Li, the contribution from Λ–Σ coupling is $\sim 12\%$ of the contribution from the ΛN spin-spin interaction in contrast to the 0^+, 1^+ spacings in the A = 4 hypernuclei, where the contributions are comparable in magnitude [27–30]. The calculations for the s-shell hypernuclei pick out NSC97e,f [31] from the YN potential models. The data from p-shell hypernuclei confirm this choice, although it should be kept in mind that the parametrization of the effective ΛN interaction includes some three-body effects.

The data from p-shell hypernuclei also strongly constrain the non-central interactions in relative p states (S_Λ, S_N, and T). Substantial effects of $S_N \sim -0.4$ MeV, which effectively augments the nuclear spin-orbit interaction in changing the spacing of core levels in hypernuclei, are seen in almost all the hypernuclei studied. The small value of S_Λ and the substantial value for S_N mean that the effective LS and ALS interactions have to be of equal strength and opposite sign. The LS interaction in the favored Nijmegen models, related to $(S_\Lambda + S_N)/2$, has roughly the correct strength but the ALS interaction is only about one third as strong as the LS interaction, albeit with the correct relative sign. The Nijmegen models also have weak odd-state tensor interactions that give a small positive value for $T \sim 0.05$ MeV. For the newer ESC04 interactions [32], the ALS interaction is a little stronger and the other components seem comparable to those of the favored NSC97 interactions, except for differences in the odd-state central interaction. The attractive odd-state central interaction of the ESC04 models is favored by some data on p_Λ states over the overall repulsive interaction for the NSC97 models.

The next generation of hypernuclear γ-ray spectroscopy experiments using a new Hyperball-J detector and the (K^-, π^-) reaction is being prepared for J-PARC. The spin-flip amplitudes are strong in the elementary interaction for $p_K = 1.1 - 1.5$ GeV/c and the day-one experiment [33] will be run at 1.5 GeV/c. The cross sections for spin-flip vs non-spin-flip strength will be checked by using a ^{4}He target and monitoring the γ ray from the 1^+ excited state of ${}^{4}_{\Lambda}$He. Also, the intention is to make a precise measurement of the lifetime of the first-excited $3/2^+$ state of ${}^{7}_{\Lambda}$Li using the Doppler shift attenuation method. For ${}^{10}_{\Lambda}$B, the ground-state doublet spacing will be determined unless it is smaller than 50 keV. For ${}^{11}_{\Lambda}$B, the power of a larger and more efficient detector array will be used to sort out the complex level scheme by the use of $\gamma\gamma$ coincidence measurements. Finally, a ^{19}F target will be used to measure the ground-state doublet spacing in ${}^{19}_{\Lambda}$F. The measurement on ${}^{19}_{\Lambda}$F represents the start of a program of γ-ray spectroscopy on sd-shell nuclei. In much of the first half of the sd shell, supermultiplet symmetry, SU3 symmetry, and LS coupling are still rather good symmetries. As a result, there are the same opportunities as in the p shell to emphasize certain spin-dependent components of the effective ΛN interaction by a judicious choice of target.

This work has been supported by the US Department of Energy under Contract No. DE-AC02-98CH10886 with Brookhaven National Laboratory.

References

1. O. Hashimoto, H. Tamura, Prog. Part. Nucl. Phys. **57**, 564 (2006).
2. H. Tamura et al., Phys. Rev. Lett. **84**, 5963 (2000).
3. K. Tanida et al., Phys. Rev. Lett. **86**, 1982 (2001).
4. H. Akikawa et al., Phys. Rev. Lett. **88**, 082501 (2002).
5. H. Tamura, these proceedings.
6. Y. Ma, these proceedings.
7. Y. Miura, Nucl. Phys. A **754**, 75c (2005); Ph.D Thesis, Tohoku University, 2005.
8. H. Tamura, Nucl. Phys. A **754**, 58c (2005).
9. M. Ukai et al., Phys. Rev. Lett. **93**, 232501 (2004).
10. M. Ukai et al, in preparation.
11. D.J. Millener, Nucl. Phys. A **754**, 48c (2005).
12. D.J. Millener, Lecture Notes in Physics, eds P. Bydzovsky, A. Gal, J. Mares (Springer), in press.
13. A. Gal, J.M. Soper, R.H. Dalitz, Ann. Phys. (N.Y.) **63**, 53 (1971); ibid. **72**, 445 (1972); ibid. **113**, 79 (1978).
14. R.H. Dalitz, A. Gal, Ann. Phys. (N.Y.) **116**, 167 (1978).
15. D.J. Millener, A. Gal, C.B. Dover, R.H. Dalitz, Phys. Rev. C **31**, 499 (1985).
16. V.N. Fetisov, L. Majling, J. Žofka, R.A. Eramzhyan, Z. Phys. A **339**, 399 (1991).
17. M. Ukai et al., Phys. Rev. C **73**, 012501 (2006).
18. E. Hiyama, M. Kamimura, K. Miyazaki, T. Motoba, Phys. Rev. C **59**, 2351 (1999).
19. E.H. Auerbach et al., Ann. Phys. (N.Y.) **148**, 381 (1983).
20. W. Brückner et al., Phys. Lett. B **79**, 157 (1978).
21. F.C. Barker, Aust. J. Phys. **34**, 7 (1981)
22. S. Cohen, D. Kurath, Nucl. Phys. **73**, 1 (1965).
23. E.K. Warburton. J.W. Olness, S.D. Bloom, A.R. Poletti, Phys. Rev. **171**, 1178 (1968).
24. D. Kurath, Nucl. Phys. A **317**, 175 (1979).
25. `http://www.tunl.duke.edu/nucldata/`.
26. R.E. Chrien et al., Phys. Rev. C **41**, 1062 (1990).
27. Y. Akaishi, T. Harada, S. Shinmura, K. S. Myint, Phys. Rev. Lett. **84**, 3539 (2000).
28. E. Hiyama, M. Kamimura, T. Motoba, T. Yamada, Y. Yamamoto, Phys. Rev. C **65**, 011301 (2001).
29. A. Nogga, H. Kamada, W. Glöckle, Phys. Rev. Lett. **88**, 172501 (2002).
30. H. Nemura, Y. Akaishi, Y. Suzuki, Phys. Rev. Lett. **89**, 142504 (2002).
31. Th.A. Rijken, V.J.G. Stoks, Y. Yamamoto, Phys. Rev. C **59**, 21 (1999).
32. Th.A. Rijken, Y. Yamamoto, Phys. Rev. C **73**, 044008 (2006).
33. J-PARC 50-GeV PS proposal E13, `http://j-parc.jp/NuclPart/pac_0606/pdf/p13-Tamura.pdf`.